

# Interconnect Structures for High-Speed Long-Distance Signal Transmission

Masanori Hashimoto Daisuke Hiramatsu Akira Tsuchiya Hidetoshi Onodera  
{hasimoto, daisuke, tsuchiya, onodera}@vlsi.kuee.kyoto-u.ac.jp

*Abstract*—This paper studies interconnect structures for long-distance signal transmission that exploits transmission line effects. We take up two basic structures, micro-strip and coplanar lines, and examine attenuation property and inductive coupling noise. We experimentally reveal that the relationship between interconnect length and required interconnect resource in 35nm and 130nm technologies. We can see that the interconnect size required for 10mm signal transmission is somewhat larger than that of the current top-metal interconnects.

## I. INTRODUCTION

In recent high-performance chip design, interconnect inductance is no longer negligible, and the interconnects that should be treated as transmission lines appear on current LSIs [1]. Recently high-speed signal transmission exploiting transmission line effects are discussed [2, 3]. The most novel advantage is the signaling speed of electro-magnetic waves independent of interconnect length. Modeling on-chip transmission lines by measurement and simulation is widely studied (well surveyed in Ref. [4]). The previous papers discuss the modeling of the given interconnect structures and/or the interconnect structures that can realize signal transmission for the given transmission length. The comprehensive study on the relationship between signal transmission length and interconnect resource required for high-speed signal transmission, that is interconnect width, thickness and spacing, has not been done.

The problems interfering with long-distance signal transmission in lossy transmission lines are attenuation and inductive coupling. As electro-magnetic waves propagate, the magnitude of the waves attenuate, and the voltage transmitted to the next-stage gate decreases. When the input voltage becomes below the logical threshold voltage, signals are not transmitted at the speed of electro-magnetic waves any longer. Inductive coupling causes crosstalk noise, which may result in logical failure and/or timing violation. This paper investigates interconnect structures for high-speed long-distance signal transmission from the view point of both attenuation and inductive coupling.

This paper is organized as follows. Sec. II discusses the requirements for high-speed long-distance signal transmission. Sec. III investigates interconnect structures with a single signal line from the viewpoint of attenuation. Sec. IV studies interconnect structures with two signal interconnects considering attenuation and coupling. Finally, Sec. V concludes the discussion.

## II. INTERCONNECT PROPERTIES FOR HIGH-SPEED SIGNAL TRANSMISSION

This section explains two essential properties to prevent high-speed signal transmission in transmission lines; attenuation and

All authors are with Dept. Communications and Computer Engineering, Kyoto University. M. Hashimoto is with PRESTO, Japan Science and Technology Corporation(JST).

inductive coupling. Reference [5] indicates the two conditions that interconnects behave as transmission lines; 1) attenuation is adequately low, 2) reactance of interconnect inductance is considerably larger than interconnect resistance and driver resistance. In this paper, we evaluate enough fat and long interconnects that satisfy the above conditions.

In transmission lines, the magnitude of a traveling wave decreases exponentially as the wave propagates. Attenuation constant  $\alpha$  is represented as follows [5].

$$\alpha \simeq \frac{R}{2} \sqrt{\frac{C}{L}} \quad (R \ll \omega_s L), \quad (1)$$

where interconnect resistance, inductance and capacitance per unit length are  $R$ ,  $L$  and  $C$ .  $\omega_s$  is  $2\pi f_s$  where  $f_s$  is the significant frequency of the traveling wave [5]. The significant frequency is expressed as  $0.34/t_r$ , where  $t_r$  is the rise transition time of the trapezoidal pulse.  $R$  and  $L$  are dependent on signal frequency. We extract the values of  $R$  and  $L$  at the significant frequency  $f_s$  using a three-dimensional extraction tool [6]. Signal attenuation is mainly caused by interconnect resistance, and hence signal attenuates drastically when interconnects become narrow and resistance  $R$  increases. Even interconnects are wide and  $R$  is small, signal attenuation of long transmission lines on LSIs can not be ignored. We here assume that the allowable attenuation for one way propagation is 50%. In CMOS circuits, the end of a transmission line is regarded as open. At an open end, a wave reflects completely and the voltage at the end becomes twice as much as the voltage of the forward wave at the end. The condition that the magnitude attenuation of the forward wave is below 50% means that the swinging voltage at the far-end is larger than the voltage injected into the near-end. This condition is expressed as follows.

$$l < -\ln 0.5/\alpha. \quad (2)$$

We evaluate this right term as the maximum interconnect length  $l_{\max}$ .  $l_{\max}$  is expressed as follows as far as the approximation in Eq. (1) holds.

$$l_{\max} \simeq \frac{1.39}{R} \sqrt{\frac{L}{C}} \quad (R \ll \omega_s L). \quad (3)$$

When there are multiple signal interconnects, mutual inductance and coupling capacitance exist. Inductive coupling between interconnects is strong when mutual inductance is large. Coupling coefficient  $K$  represents the strength of inductive coupling and is expressed as

$$K = \frac{M_{12}}{\sqrt{L_1 L_2}}, \quad (4)$$

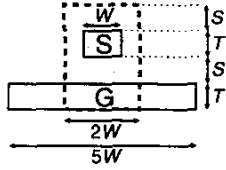


Fig. 1. Micro-strip structure.

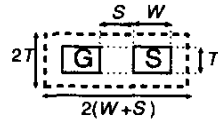


Fig. 2. Coplanar structure.

where  $L_1$  and  $L_2$  are the self inductances of two interconnects and  $M_{12}$  is the mutual inductance. When a signal transition occurs at one interconnect, crosstalk noise appears at the other interconnect. Generally speaking, crosstalk noise tends to be large as coupling becomes strong. Then coupling coefficient should be small. We discuss the relationship between coupling coefficient  $K$  and the magnitude of crosstalk noise in Sec. IV-A.

### III. LOW-ATTENUATION INTERCONNECT STRUCTURES

We assume two basic structures of micro-strip and coplanar, and evaluate them from the point of attenuation. Figs. 1 and 2 show the cross section of interconnects. "S" in the figures corresponds to a signal interconnect and "G" is a ground interconnect. We here evaluate a single signal interconnect with a ground line surrounded with no signal interconnects. The interconnect structures with two signal interconnects are evaluated in the next section. Interconnect resistance  $R$ , inductance  $L$  and capacitance  $C$  are evaluated varying interconnect width  $W$ , thickness  $T$  and distance from ground  $S$  [6]. Skin effect and proximity effect are considered.  $L$  is loop inductance when the ground interconnect is assigned to the return path. We assume a 35nm technology in 2014 predicted in ITRS roadmap [7]. Resistivity of interconnects is  $1.8 \times 10^{-8} \Omega\text{m}$  and relative dielectric constant of interlevel metal insulator is 1.5. We use a transistor model that is available on Web site [8]. This transistor model is generated such that current-voltage characteristic fits to that predicted in ITRS roadmap [7]. We use the signal transition time of an inverter with fanout 4 load to decide significant frequency. In this technology, the transition time is 11.5ps and the significant frequency is 30.5GHz.

#### A. Relationship between Interconnect Length and Interconnect Resource

Fig. 3 demonstrates the relationship between interconnect resource and the maximum interconnect length  $l_{\max}$ . We assume  $S = T = 1.5W$  in the micro-strip structure and  $S = W = 1.5T$  in the coplanar structure. We here choose the interconnect structures whose capacitance  $C$  is small because the maximum interconnect length  $l_{\max}$  becomes small when capacitance  $C$  increases from Eq.(3). Interconnect resource is evaluated as the section area that a pair of signal and ground interconnects occupy. The section area is shown in Figs. 1 and 2, and is represented as  $4W(S+T)$  in the micro-strip structure and  $4S(W+T)$  in the coplanar structure. Here, these results are an example because the maximum interconnect length  $l_{\max}$  can not be decided deterministically according to the section area. From Fig. 3, we can see that the required interconnect resource increases exponentially as the interconnect length increases. The required interconnect resource of the coplanar structure is larger than that of the micro-strip structure. This is because the resistance of the

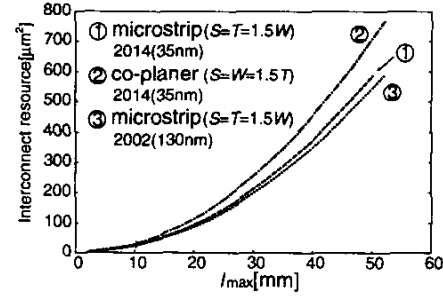


Fig. 3. Relationship between maximum interconnect length  $l_{\max}$  and required interconnect resource.

ground interconnect is large in the coplanar structure.

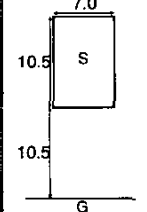
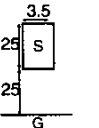
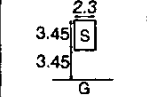
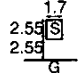
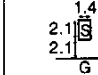
The similar evaluation is made assuming a 130nm technology in 2002 predicted in ITRS roadmap [7]. In this technology, resistivity is  $2.2 \times 10^{-8} \Omega\text{m}$ , relative dielectric constant is 3.5, the signal transition time is 35.0ps and the significant frequency is 10GHz. Fig. 3 demonstrates no distinct difference of attenuation in both technologies. Compared with the 35nm technology, the interconnect capacitance is over twice as large because of the large dielectric constant. However, the significant frequency is about one-third and skin effect is not dominant. Therefore the interconnect resistance is small. The increase of capacitance is compensated by the low interconnect resistance. Hereafter we evaluate interconnect structures assuming the 35nm technology.

#### B. Tradeoff of Repeater Insertion between Interconnect Resource and Propagation Delay

We suppose 50mm signal transmission with repeater insertion. Table I shows the relationship between the number of inserted repeaters and the required interconnect resource in the micro-strip structure. When no repeaters are inserted in a 50mm interconnect, the interconnect width  $W$ , thickness  $T$ , and distance to ground  $S$  should be 7.0, 10.5 and  $10.5 \mu\text{m}$  respectively. The interconnect resource is  $4W(S+T) = 588 \mu\text{m}^2$ . When one repeater is inserted and the interconnect length for one driver becomes 25mm,  $W$ ,  $T$ ,  $S$  and  $4W(S+T)$  are reduced to 3.5, 5.25,  $5.25 \mu\text{m}$  and  $147 \mu\text{m}^2$ . The required interconnect resource is reduced by 75%. When four repeaters are inserted and the interconnect length for a driver is 10mm,  $W$ ,  $T$ ,  $S$  and  $4W(S+T)$  become 1.4, 2.1,  $2.1 \mu\text{m}$  and  $23.5 \mu\text{m}^2$ . The required interconnect resource is reduced to only 4% of the resource without repeaters.

Signal propagation speed in transmission lines is constant independent of interconnect length. The signal propagation delay increases by the inserted repeater delay, although repeater insertion reduces the required interconnect resource. We evaluate the signal propagation delay from the driver input to the interconnect end in the interconnect structures shown in Table I. The propagation delay is estimated by circuit simulation using the RLC interconnect model in Fig. 4. The driver and repeaters are inverters whose driving strength are the same. The driver strength is decided such that the equivalent output resistance becomes the half of the characteristic impedance of the transmission line. In this case, the voltage injected into the interconnect is 67% of supply voltage. From the definition of maximum interconnect length  $l_{\max}$ , the voltage magnitude at the far-end is

TABLE I  
AN EXAMPLE OF INTERCONNECT RESOURCES REQUIRED FOR 50MM  
SIGNAL TRANSMISSION.

#Repeaters	0	1	
Length for a driver[mm]	50.0	25.0	
Characteristic impedance[Ω]	97.8	99.9	
Interconnect resource[μm <sup>2</sup> ]	588	147	
Propagation delay[ps]	226	246	
Cross section (Unit is μm.)			
	2	3	4
	16.7	12.5	10.0
	102	104	106
	63.5	34.9	23.5
	266	283	307
			

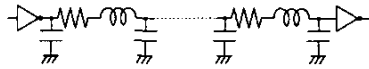


Fig. 4. RLC interconnect model.

the same with the voltage injected into the interconnect at the near-end. This condition on the driving strength means that the input voltage of the next stage gate swings by 67% of supply voltage.

Table I lists the evaluation results. The signal propagation delay increases because of the inserted repeater delay. The delay of a repeater is about 20ps, The speed of electric-magnetic wave is expressed as  $v = c_0/\sqrt{\epsilon}$  and the speed in this technology is  $2.45 \times 10^8$  m/s, where  $\epsilon$  is the relative dielectric constant of interlevel metal insulator and  $c_0$  is the light speed. The theoretical propagation delay of 50mm interconnect, which excludes the delay of the driver and the repeaters, is 204ps and is consistent with the circuit simulation results. The delay increase of one repeater insertion corresponds to the delay increase of 10%, and it is small compared with the reduction ratio of the required interconnect resource.

#### IV. LOW COUPLING INTERCONNECT STRUCTURES

The previous section evaluates the structure with a signal and a ground interconnects. On actual LSIs, multiple signal interconnects are adjacently routed in parallel, and hence we need to consider the influence of the neighboring interconnects. Mutual inductance and coupling capacitance exist among interconnects, and hence crosstalk noise appears. Also, the maximum interconnect length is different from the evaluation result for a single signal interconnect, because the interconnect resistance, capacitance, and inductance are dependent on the distance to neighbor interconnects. In this section, we investigate interconnect structures for high-speed signal transmission considering neighboring interconnects.

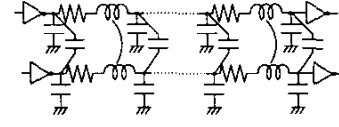


Fig. 5. Coupled RLC interconnects.

#### A. Relation between Interconnect Parameters and Noise

Coupling coefficient is closely related to magnitude of crosstalk noise [1]. However other factors also affect crosstalk noise to a certain degree. We here discuss the relation between interconnect characteristics and crosstalk noise, and we reveal the relationship between coupling coefficient and noise magnitude considering other interconnect properties. The interconnect parameters are interconnect length  $l$ , resistance  $R$ , inductance  $L$  and capacitance  $C$ . When two adjacent interconnects are considered, there are mutual inductance and coupling capacitance as well as the values of  $l$ ,  $R$ ,  $L$  and  $C$  of the other interconnect. When we suppose that the width, thickness and length of two interconnects are the same, the resistances are almost the same, though proximity effect varies  $R$  rigidly. Inductance  $L$  is in inverse proportional to capacitance  $C$ , and hence the variation of  $L$  and  $C$  is represented as that of the characteristic impedance  $Z_0 = \sqrt{L/C}$ . The relation between two signal interconnects are expressed as coupling coefficient  $K = M_{12}/\sqrt{L_1 L_2}$  and inductance ratio  $L_2/L_1$ . Driver strength is commonly decided for impedance matching. We then evaluate crosstalk noise of the interconnects driven by impedance-matched gates. From the above discussion, we choose five parameters, interconnect length  $l$ , characteristic impedance  $Z_0$ , resistance  $R$ , inductance ratio  $L_2/L_1$  and coupling coefficient  $K$ , and evaluate crosstalk noise under various values of them.

We here evaluate the magnitude of the noise,  $V_{\text{noise}}$ , that appears at the far-end of one interconnect when a signal transition occurs at the other interconnect. The noise is estimated by circuit simulation using the coupled RLC interconnect model shown in Fig. 5. The values of  $R$ ,  $C$  and  $L$  are varied assuming certain interconnect structures, which means that impractical variations are excluded for noise evaluation.

$l$ ,  $K$  and  $V_{\text{noise}}$  We first assume  $Z_0 = 105\Omega$ ,  $R = 7.56\Omega$ ,  $K = 0.30$ , and  $L_2/L_1 = 1$ . The curve of ② in Fig. 6 represents the relationship between the interconnect length and the magnitude of crosstalk noise. The horizontal axis represents the interconnect length normalized by multiplication of  $R/Z_0$ . This normalization makes the maximum interconnect length  $l_{\text{max}}$  corresponding to 1.39 of  $R/Z_0$  (Eq 3). The vertical axis is  $V_{\text{noise}}/V_{\text{DD}}$ . As  $l$  increases,  $V_{\text{noise}}$  becomes large and have the peak value around  $R/Z_0 = 1.5$ . We next vary  $K$  to 0.20, 0.40 and 0.50, and evaluate crosstalk noise with  $R$ ,  $Z_0$ ,  $L_2/L_1$  almost unchanged. The curves of ①, ③ and ④ correspond to the results in order respectively. The magnitude of crosstalk noise increases proportionally to  $K$ , whereas the shapes of the curves are similar to the curve of ②.

$Z_0$  and  $V_{\text{noise}}$  Crosstalk noise is evaluated under three variations of  $Z_0$ ; 60.5Ω, 105Ω and 130Ω. Though the values of  $Z_0$  are different,  $R$ ,  $K$  and  $L_2/L_1$  are almost the same for three interconnect structures. The curve of  $V_{\text{noise}}$  is similar to the curves in Fig. 6.  $V_{\text{noise}}$  becomes small as  $Z_0$

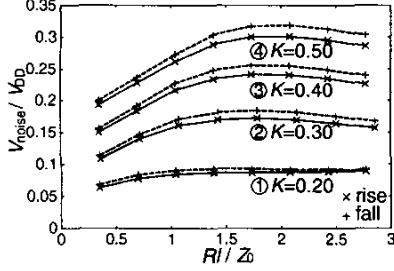


Fig. 6. Relationship between noise magnitude  $V_{\text{noise}}$  and interconnect length  $l$  ( $K = 0.20, 0.30, 0.40, 0.50$ ).

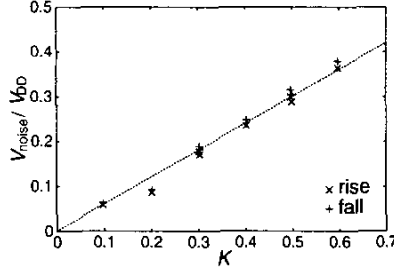


Fig. 7. Relation between coupling coefficient  $K$  and noise magnitude  $V_{\text{noise}}$ .

increases. However the amount of difference is 20% and is not so large between the structures of  $Z_0 = 60.5\Omega$  and  $Z_0 = 130\Omega$ .

**$R$  and  $V_{\text{noise}}$**  We change  $R$  to  $3.66\Omega$ ,  $7.56\Omega$ ,  $16.2\Omega$  with  $Z_0$ ,  $K$  and  $L_2/L_1$  unchanged. The relationship between  $l$  and  $V_{\text{noise}}$  is similar to Fig. 6.  $V_{\text{noise}}$  becomes large as  $R$  decreases. However the difference is relatively small and about 20% between  $R = 7.56\Omega$  and  $R = 3.66\Omega$ .

**$L_2/L_1$  and  $V_{\text{noise}}$**  We evaluate crosstalk noise for the non-symmetric interconnect structures. The variations of  $L_2/L_1$  are 0.74, 1 and 1.45.  $Z_0$ ,  $R$  and  $K$  are almost the same for all structures. The relationship between  $l$  and  $V_{\text{noise}}$  are the same with Fig. 6. The magnitude of crosstalk noise are almost the same for three conditions of  $L_2/L_1$ .

Summalizing the above results, the magnitude of crosstalk noise  $V_{\text{noise}}$  is mainly determined by coupling coefficient  $K$ . Comared with  $K$ , interconnect length  $l$ , characteristic impedance  $Z_0$ , resistance  $R$  and inductance ratio  $L_2/L_1$  affects crosstalk noise slightly. The second most dominant parameter to  $V_{\text{noise}}$  is  $l$ . The relation between  $l$  and  $V_{\text{noise}}$  does not change so much in spite of the variation of other parameters. The maximum variation of  $V_{\text{noise}}$  is at most 40%. We here assume that interconnect length  $l$  is smaller than the maximum length  $l_{\text{max}}$  defined in Sec. II. From Eq. (3),  $Rl/Z_0$  becomes 1.39 when  $l = l_{\text{max}}$ . We can see from Fig. 6 that  $V_{\text{noise}}$  increases monotonically in the regin of  $Rl/Z_0 < 1.39$ . We therefore evaluate the magnitude of crosstalk noise  $V_{\text{noise}}$  when  $l = l_{\text{max}}$ .

We choose the evaluation results under the condition of  $l = l_{\text{max}}$ , i.e. under the condition of  $Rl/Z_0 = 1.39$ , and plot them in Fig. 7. As you see, the magnitude of crosstalk noise  $V_{\text{noise}}$  increases linearly as coupling coefficient  $K$  becomes large. From Fig. 7, we can estimate  $V_{\text{noise}}$  on the condition that the estimated value may change by  $\pm 20\%$  according to interconnect structures.

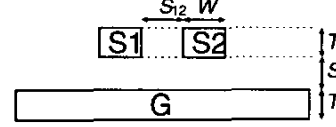


Fig. 8. Micro-strip structure with two signal interconnects.

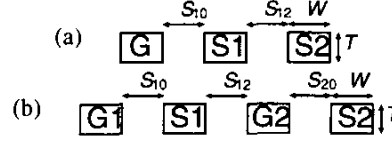


Fig. 9. Coplanar structure with two signal interconnects.

## B. Coupling Coefficient Evaluation

We here evaluate coupling coefficient for various interconnect structures with two signal interconnects. The previous section reveals that coupling coefficient are tightly related to the magnitude of crosstalk noise and their relation is linear. When we suppose that the crosstalk noise whose magnitude is the quarter of supply voltage is allowable, the coupling coefficient  $K$  should be below 0.40(Fig. 7). We assume that two signal interconnects S1 and S2 are in parallel at the distance  $S_{12}$ . Fig. 8 represents the assumed micro-strip structure and Fig. 9(a) is the coplanar structure.

Fig. 10 demonstrates the variation of  $K$  in the micro-strip structure varying the distance  $S_{12}$  when  $W = 2.0\mu\text{m}$ ,  $T = 2.0\mu\text{m}$ ,  $S_0 = 2.0\mu\text{m}$ . In order to reduce  $K$  to below 0.40, the spacing  $S_{12}$  should be over  $2.0\mu\text{m}$ . Coupling coefficient  $K$  is sensitive to  $S_{12}$ , and  $K$  decreases by 50% when  $S_{12}$  becomes twice. The increase of  $S_{12}$ , however, means degradation of interconnect density and is not desirable.

Fig. 11 demonstrates the evaluation results for the coplanar structure. Coupling coefficient  $K$  stays almost unchanged though  $S_{12}$  increases. In order to realize  $K$  of 0.4, the distance  $S_{12}$  should be as much as  $14\mu\text{m}$ . In the coplanar structure, adjoining singal interconnects are prohibited from the point of inductive coupling.

We then assume the coplanar structure shown in Fig. 9(b). A ground interconnect G2 is inserted between the signal interconnects S1 and S2. Fig. 12 shows the relationship between  $K$  and  $S_{12}$  assuming  $S_{10} = S_{20} = W = 2.0\mu\text{m}$ . Coupling coefficient  $K$  is reduced to one-fifth compared with the structue without G2. Inserting a ground interconnect G2 helps to reduce inductive coupling considerably. In this case,  $K$  is about 0.12.  $K$  is insensitive to  $S_{12}$  and does not change so much.

From the above discussion,  $K$  in the micro-strip structure considerably depends on the distance between the signal interconnects. Coupling coefficient  $K$  of 0.4 can be realized by increasing the distance. On the other hand, in the coplanar structure, inductive coupling is excessively strong when signal interconnects are adjacent. Inserting a ground interconnect between signal interconnects is necessary. In that strcutre, the coupling coefficient  $K$  is about 0.12 and one-fifth of that without the ground interconnect. Hereafter, we assume the coplanar structure of Fig. 9(b).

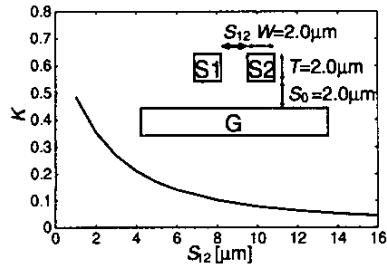


Fig. 10. Relationship between  $K$  and  $S_{12}$  (micro-strip,  $W = 2.0\mu\text{m}$ ,  $T = 2.0\mu\text{m}$ ,  $S_0 = 2.0\mu\text{m}$ ).

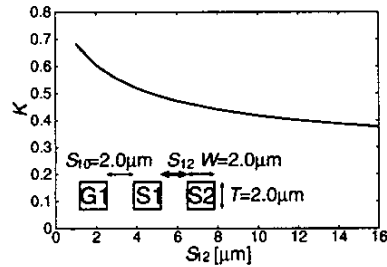


Fig. 11. Relationship between  $K$  and  $S_{12}$  (coplanar of Fig. 9(a),  $W = 2.0\mu\text{m}$ ,  $T = 2.0\mu\text{m}$ ,  $S_{10} = 2.0\mu\text{m}$ ).

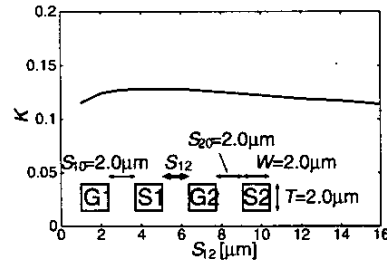


Fig. 12. Relationship between  $K$  and  $S_{12}$ . (coplanar of Fig. 9(b),  $W = S_{10} = S_{20} = 2.0\mu\text{m}$ ,  $T = 2.0\mu\text{m}$ ).

### C. Required Interconnect Resource

When there are neighboring signal interconnects, interconnect resistance, capacitance and inductance are different from those without adjacent signal interconnects, which makes the maximum interconnect length  $l_{\text{max}}$  different. We here examine the required interconnect resource considering both attenuation and crosstalk noise.

We first evaluate the micro-strip structure for 10mm signal transmission. We assume  $S_0 = T = 1.5W$  similarly to the previous section. We derive the ratio of  $S_{12}/W$  that makes coupling coefficient  $K$  below 0.40, and decide the interconnect structure for 10mm transmission. Fig. 13 shows the derived interconnect structure. The required interconnect width is 1.15 times as large as that for a single signal interconnect, because interconnect capacitance is larger due to coupling capacitance. Coupling coefficient  $K$  is 0.39 when distance  $S_{12}$  is  $2.4\mu\text{m}$ .

We also evaluate the interconnect structure with coupling coefficient  $K$  of below 0.20 supposing coupling noise constraint is more tight. From Fig. 7,  $K$  of 0.20 corresponds to the noise whose magnitude is 12% of supply voltage. Under this condition, the required distance  $S_{12}$  is  $5.6\mu\text{m}$  and is four times larger than the interconnect width  $W$ . As Fig. 10 demonstrates, the required distance  $S_{12}$  becomes large.

We next discuss the coplanar structure. We assume  $S_{10} =$

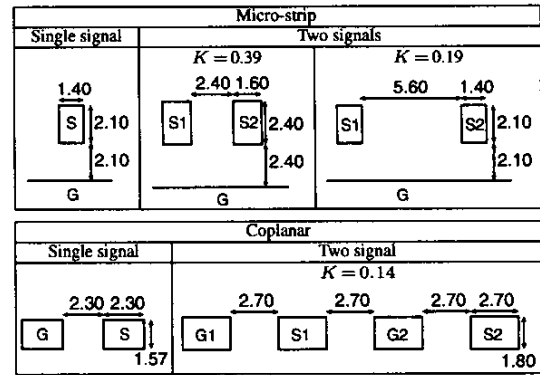


Fig. 13. An example of interconnect structure for 100mm signal transmission. (Unit length is  $\mu\text{m}$ ).

$W = 1.5T$  similarly to the previous section. We suppose  $S_{10} = S_{20} = S_{12} = W$  because the distance between  $S_1$  and  $G_2$  scarcely affects  $K$  as shown in Fig. 12. Fig. 13 demonstrates the derived interconnect structure for 10mm transmission. The interconnect thickness and width of the coplanar structure are somewhat larger than those of top-layer metal of  $0.13\mu\text{m}$  technologies. In this time,  $K$  is 0.14 and corresponds to the noise whose magnitude is 8% of supply voltage.

### V. CONCLUSION

We study interconnect structures from the standpoint of transmission lines, and derive some structures for high-speed long-distance signal transmission in 130nm and 35nm technologies as an example. Through this study, we can see the following five things: 1) Required interconnect dimensions increase exponentially as interconnect length increases. 2) The interconnect resource for 10mm signal transmission is slightly larger than that of current top-metal layer interconnects. 3) Magnitude of crosstalk noise is well expressed by coupling coefficient. 4) Increasing distance between signal interconnects in micro-strip structures reduces coupling coefficient, i.e. crosstalk noise. 5) Crosstalk noise of adjoining interconnects in coplanar structure excessively large and ground interconnects must be inserted between signal interconnects.

### REFERENCES

- [1] A. Deutsch, P. W. Coteus, G. V. Kopcsay, H. H. Smith, C. W. Surovic, B. L. Krauter, D. C. Edelstein and P. J. Restle, "On-Chip Wiring Design Challenges for Gigahertz Operation," *Proc. IEEE*, Vol. 89, No.4, April 2001.
- [2] M. Mizuno, K. Anjo, Y. Sumi, H. Wakabayashi, T. Mogami, T. Horiuchi and M. Yamashina, "On-Chip Multi-GHz Clocking with Transmission Lines," *Proc. ISSCC*, pp.366-367, 2000.
- [3] R. T. Chang, C. P. Yue and S. Simon Wong, "Near Speed-of-Light On-Chip Electrical Interconnect," *Proc. Symposium on VLSI Circuits*, to appear.
- [4] A. Deutsch, G. V. Kopcsay, C. W. Surovic, B. J. Rubin, L. M. Terman, R. P. Dunne Jr., T. A. Gallo and R. H. Dennard, "Modeling and Characterization of Long On-Chip Interconnections for High-Performance Microprocessors," *IBM Journal of Research and Development*, Vol. 39, No. 5, pp.547-567, 1995.
- [5] Chung-Kuan Cheng, John Lillis, Shen Lin, Norman H. Chang, "Interconnect Analysis and Synthesis," A Wiley-Interscience Publication., 2000.
- [6] "Raphael User Manual," Avant! Corp., 1998.
- [7] International Technology Roadmap for Semiconductors 1999, SIA, Semantech Inc., 1999.
- [8] K. Inagaki, K. Kanda, T. Sakurai, "Organization of a Standard SPICE Model based on International Technology Roadmap for Semiconductors," <http://lowpower.iis.u-tokyo.ac.jp/~ina/index.html>, 2000.